Surface & Coatings Technology 370 (2019) 1–10

Contents lists available at ScienceDirect

Surface & Coatings Technology

journal homepage: www.elsevier.com/locate/surfcoat

Effect of glassy carbon, gold, and nickel electrodes on nickel electrocrystallization in an industrial electrolyte

Yangtao Xu, Kai Huang*, Zhenxu Zhu, Tiandong Xia

State Key Laboratory of Advanced Processing and Recycling of Non-ferrous Metal, Lanzhou University of Technology, Lanzhou, Gansu 730050, China
School of Materials Science and Engineering, Lanzhou University of Technology, Lanzhou, Gansu 730050, China

ARTICLE INFO

Keywords:
Nickel electrocrystallization
Industrial electrolyte
Glassy carbon electrode
Gold electrode
Nickel electrode

ABSTRACT

The effects of three different substrate materials (glassy carbon, gold, and nickel electrodes) on the electrocrystallization behavior of nanocrystalline nickel in an industrial electrolyte with complex compositions were studied by cyclic voltammetry (CV), single potential step chronoamperometry. The CV results indicated that the initial deposition potentials of nickel shift to the positive direction in the order glassy carbon < gold < nickel electrodes, while the nickel deposition overpotential decreased at the same time. Chronoamperometry results indicated that from the glassy carbon to gold and nickel electrodes, the adhesion of nickel nanoparticles on the electrodes increased, nucleation relaxation time became shorter, and the number of nuclei decreased. As the deposition potential is negatively shifted and the deposition time is prolonged, the *I-t* curves for the nickel and gold electrodes are more stable and reliable than those from the glassy carbon electrodes. The chronoamperometric study combined with SEM revealed that the nucleation mechanism of nickel on different substrates changed from three-dimensional progressive to instantaneous, but the time of the transition is different. When the deposition time is 100 s, the nanocrystalline nickel deposited on the nickel and gold electrodes has good integrity and uniformity. This was also confirmed in studies using atomic force microscopy and transmission electron microscopy. Moreover, the results of transmission electron microscopy (TEM) show that there are many twins in the nanocrystalline nickel layer deposited on the gold electrode at −0.95 V, 100 s. The electrocrystallization process of nickel is complicated by the complex ionic components in the industrial electrolyte of the nickel sulfide soluble anode/mixed acid system.

1. Introduction

Nickel has good physical and chemical properties and is widely used in improving the performance of high-precision materials, surface protection, and other fields. Nickel starting sheet is commonly used as the substrate in industrial electrolytic nickel production. The industrial electrolyte of nickel sulfide soluble anode/mixed acid system used for electrocrystallization of nickel has a complex composition, containing many metal ions including impurity ions (such as Cu^{2+}, Ni^{2+}, Cl^{-}, Na^{+}, Fe^{2+}, Co^{2+}, and Zn^{2+}) [1–4]. The growth morphology of nickel electrocrystallines is affected by not only the electrodeposition conditions, but also the substrate orientation [5,6]. Therefore, under certain sedimentary conditions, sedimentary layers with the same composition and structure will display different external morphology according to the substrates. To observe the growth morphology during electrocrystallization, experiments are usually carried out on single-crystal electrodes with the same composition as the deposited metal [7,8]. However, due to the influence of experimental cost (the current sales prices of gold, glassy carbon, copper, low carbon steel and nickel electrodes decreased in turn) and research system, the choice of electrodes should be determined for each specific situation.

There have been many reported studies on electrocrystallization. For example, Abyaneh et al. [9–11] proposed an electrocrystallization model and derived the transient equation of the electric current. Gomez et al. [12–16] studied the initial behavior of nickel electrocrystallization using constant potential step technology and cyclic voltammetry (CV). It was found that at low overpotentials nickel electrocrystallization followed the three-dimensional continuous nucleation/growth mechanism, while at high overpotentials it followed the three-dimensional instantaneous nucleation/growth mechanism. Zhang et al. [17] studied the effect of valine on the electrocrystallization process of nickel on glassy carbon electrodes, and Lantelme et al. [18] also

* Corresponding author at: State Key Laboratory of Advanced Processing and Recycling of Non-ferrous Metal, Lanzhou University of Technology, Lanzhou, Gansu 730050, China.
E-mail address: nxhk2018@163.com (K. Huang).

https://doi.org/10.1016/j.surfcoat.2019.04.072
Received 7 March 2019; Received in revised form 18 April 2019; Accepted 23 April 2019
Available online 24 April 2019
0257-8972/

analyzed the constant potential current-time transient curves of nickel nucleation and growth on glassy carbon. The results show that nickel deposition in acidic solution conforms to the nucleation and hemispherical growth mechanism. Li et al. [19] studied the electrocrystallization mechanism of nickel in sodium citrate solution using a glassy carbon electrode. Xu et al. [20] studied the microstructure and texture evolution of electrodeposited coatings of nickel in the industrial electrolyte. Nitin et al. [21] proposed a new model for predicting the grain size of electrodeposited nanocrystalline nickel coatings containing sulphur, phosphorus or boron based on typical systems, and deals with influence of current density and impurities on grain size of Ni. However, some reports claimed that the glassy carbon electrode has great limitations in studying nickel electrocrystallization, while there have been few studies on nickel electrocrystallization using metal electrodes such as gold and nickel electrodes. As the same time, the studies on nucleation and growth of nickel in industrial electrolytes of soluble anode/mixed acid system of nickel sulfide have not been reported.

Based on these considerations, in order to select a suitable working electrode to study the electrocrystallization process of nickel in industrial electrolytes, in this study we examined the effect of different substrates (glassy carbon, gold, and nickel electrodes) as working electrodes on the electrocrystallization behavior of nanocrystalline nickel. Considering the practical applications, we directly used the industrial electrolyte of nickel sulfide soluble anode/mixed acid system sampled from an industrial production line, which has a more complex composition than simple electrolytes prepared in the laboratory.

2. Experimental

Electrochemical studies were performed with a typical three-electrode cell (the three-electrode system can more accurately measure the potential and potential changes of different working electrodes) connected to an electrochemical workstation (multichannel system PARSTAT MC). The experimental temperature was kept at room temperature by a thermostatic device. The working electrodes were a glassy carbon, a gold, and a nickel electrode all with the diameter of 4.0 mm. The auxiliary electrode is a platinum electrode with a size of 1.0 cm × 1.0 cm. A saturated calomel electrode (SCE) serves as reference electrode, and all potentials reported here are expressed with respect to the SCE.

The industrial electrolyte of the nickel sulfide soluble anode/mixed acid system ((hereinafter referred to as industrial electrolyte) was sampled from a domestic company's production line. With a solution pH of 5.3, the composition of the industrial electrolyte is shown in Table 1. Sulfuric acid (H_2SO_4), potassium chloride (KCl), and potassium ferricyanide ($K_3[Fe(CN)_6]$) used in the experiments were all analytical pure chemical reagents. Pure water (> 10 MΩ·cm) was used in the experiments.

Before each experiment, the working electrodes were pretreated by the following steps. The gold and nickel electrodes were polished by 2500, 3000, and 5000 mesh metallographic sandpaper, the glassy carbon electrode was polished by 5000 mesh metallographic sandpaper, and mechanically polished to a nearly mirror surface finish with 0.05 μm finer grades of alumina powders. Then, the electrode surface was rinsed thoroughly under distilled water. The gold electrode was acid pickled with a mixed solution of concentrated sulfuric acid and hydrogen peroxide (3:1 by volume), the glassy carbon electrode was acid pickled with 0.1 mol/L concentrated sulfuric acid, and then rinsed with pure water (repeat three times). Because the surface of nickel electrode will be damaged by acid pickling, it is not necessary to carry out acid pickling on the surface of nickel electrode. The glassy carbon and gold electrodes need to be tested for potassium ferricyanide to ensure meeting the requirements, which does not apply to the nickel electrode. All three types of working electrodes were ultrasonically cleaned with pure water, absolute ethanol, and pure water in sequence for 3 to 5 min to remove surface impurities, and then rinsed with pure water. The gold electrode needed to be activated in 1 mol/L sulfuric acid solution until the CV curve was stable (about 20 cycles). Finally, the treated electrodes were rinsed with pure water and dried at room temperature before use.

Table 1
Composition of the industrial electrolyte.

Ni^{2+}	Cl^-	Na^+	Cu^{2+}	Fe^{2+}	Co^{2+}	H_3BO_3
75 g/L	70 g/L	40 g/L	3 mg/L	4 mg/L	20 mg/L	5 g/L

According to the obtained CV curves, the *I-t* curve was calculated in the range of −0.85 to −1.00 V by using the electric potential step technology, and the dimensionless curve of I^2/I_m^2-t/t_m from theory was drawn according to the *I-t* curve. The experimental curve was fitted using the Scharifker-Hill model, and the nucleation mechanism of Ni on glassy carbon, gold, or nickel electrodes was determined. Electrodeposition was carried out under constant current density for different substrate surfaces for a certain period of time. The morphology of the deposit was observed by atomic force microscope (AFM, CSPM5500), field emission transmission electron microscope (TEM, FEI Talos F200) and scanning electron microscopy (SEM, Quanta450FEG). (Before the SEM observation, in order to enhance the conductivity of the sample, the nickel deposit should be treated with gold spraying.)

3. Results and discussion

3.1. CV curves

Fig. 1 shows the CV curves of the nickel electrocrystallization process on the surfaces of three electrodes. In Fig. 1(a), the electric current mutation point of nickel was at −1.05, −1.00, and −0.91 V for the glassy carbon, gold, and nickel electrodes, respectively. X-ray diffraction was performed on glassy carbon, gold, nickel electrodes and nickel deposits, the X-ray diffraction patterns of glassy carbon, gold and nickel electrodes and nickel deposit layer were analyzed by JADE6 analysis software and the corresponding lattice parameters were calculated. The results show that glassy carbon is an amorphous structure. The lattice parameters of gold electrodes are a = b = c = 4.078 Å, the lattice parameters of nickel electrodes are a = b = c = 3.524 Å, and the lattice parameters of nickel deposit layer are a = b = c = 3.529 Å. Therefore, the difference of lattice parameters between nickel deposition layer and glassy carbon, gold and nickel electrodes decreases in turn. The initial nickel deposition potential was positively shifted in this order, since the lattice difference between the nickel deposit and the substrate material decreased sequentially, which redued the energy required for deposition and the deposition overpotential. Therefore, the nucleation and growth of nickel during electrocrystallization were promoted in the order of glassy carbon < gold < nickel, and the corresponding peak current of deposition in the CV curves was −10.45, −13.70, and − 11.20 mA [16]. The peak deposition current for the gold electrode was significantly higher than for the other two electrodes, indicating that the current efficiency is higher on the surface of the gold electrode.

It can be seen from Fig. 1(b) that the initial nickel deposition potential on gold and nickel electrodes is shifted positively, the deposition peak is shifted positively, and the dissolution peak is shifted negatively. The corresponding deposition/dissolution peaks are located at −1.22/−0.06 V and −1.20/−0.15 V, respectively. The electrodeposition of nickel on the surface of gold and nickel electrodes is a reduction process involving two electrons [22]. According to the illustration, the respective range of the “inductive current cycle” for the gold and nickel electrodes is −0.7198 to −0.8958 V and −0.6650 to −0.9202 V, indicating that there is an overpotential for the nucleation process during electrodeposition of nickel on these electrode surfaces. The equilibrium potential of nickel deposition on the gold and nickel electrode surfaces

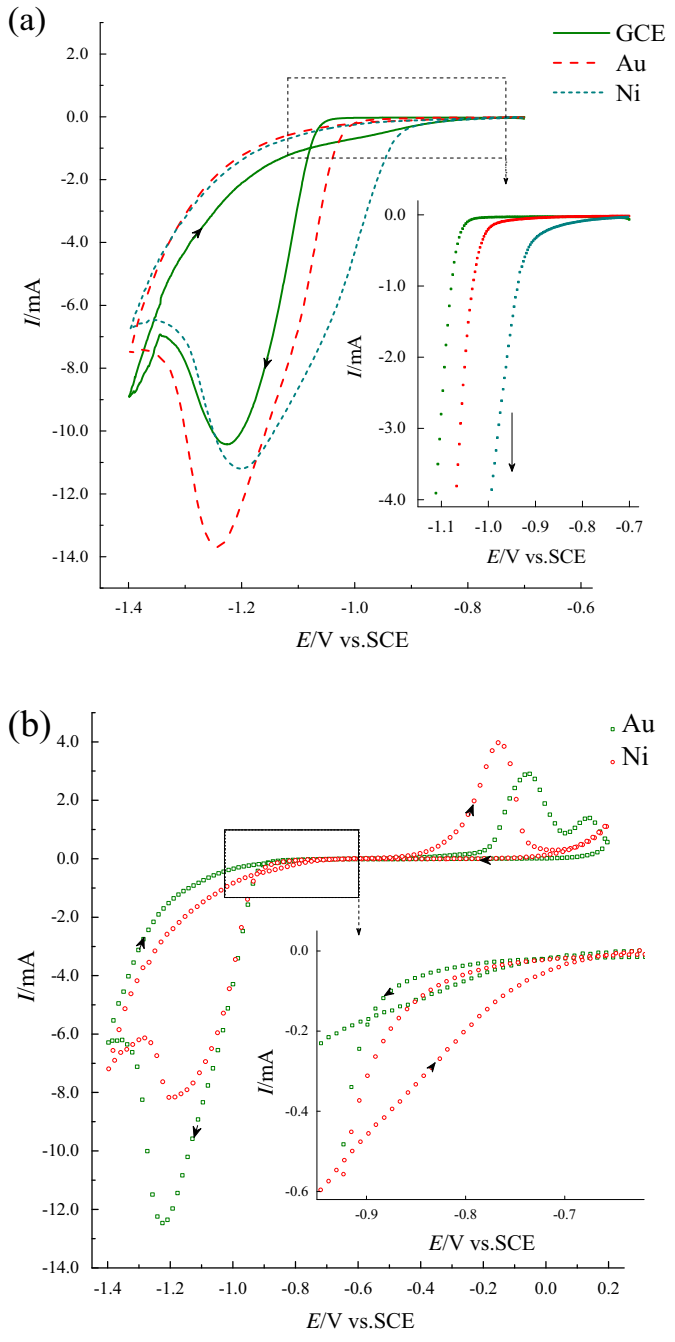

Fig. 1. Cyclic voltammograms recorded for different electrodes in industrial electrolytes at (a) 0.055 V·s^{-1} and (b) 0.040 V·s^{-1}.

is −0.7198 and −0.6650 V, and the initial deposition potential is −0.88 and −0.82 V, respectively. Therefore, the nucleation overpotential was 0.1602 for the gold electrode and 0.1550 V for the nickel electrode. In other words, the use of a nickel electrode reduces the overpotential of nickel electrocrystallization relative to the gold electrode.

By comparing Fig. 1(a) and (b), it can be found that in the cyclic voltammetry experiment, the difficulty in forming the "inductive current cycle" in the Cv curve obtained from the glassy carbon, gold and nickel electrodes is sequentially increased when the scanning speed is 0.055 V·s^{-1} (the CV curve obtained by nickel electrode under this condition did not form an "inductive current cycle"). The "inductive current cycle" in the CV curve obtained by the gold and nickel electrodes appears normally when the scanning speed becomes 0.040 V·s^{-1}.

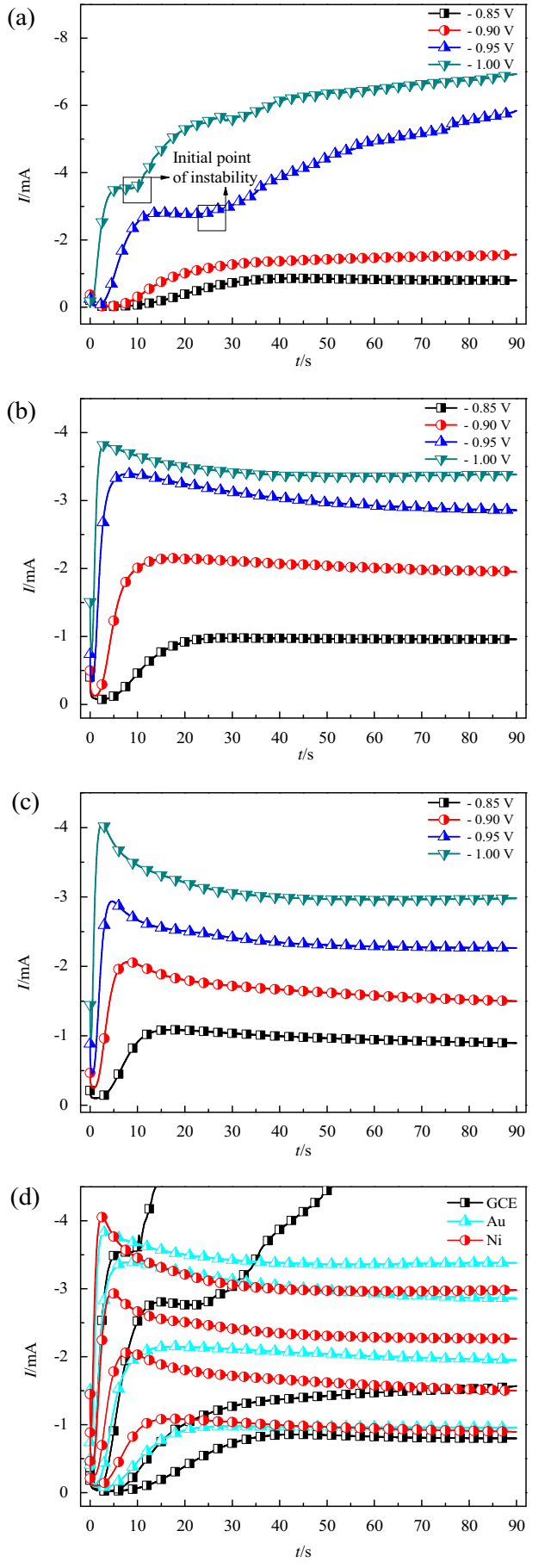

(caption on next page)

Fig. 2. Chronoamperometric curves at different step potentials on different electrodes: (a) glassy carbon electrode, (b) gold electrode, (c) nickel electrode. (d) Comparison of the three electrodes. (For interpretation of the references to colour in this figure legend, the reader is referred to the web version of this article.)

In summary, in cyclic voltammetry experiments, the extent of the effect of scanning speed on the electrocrystallization process of nickel varies with the matrix.

From the experimental cyclic V—I curves in the industrial electrolyte, it is extremely difficult for the glassy carbon electrode to display a normal deposition peak. On the gold electrode, the distribution of nickel deposit layer is not uniform, while the nickel electrode has certain limitation on the initial potential and the positive range of the potential window. Considering these facts, the gold and nickel electrodes are more suitable working electrodes for CV experiments in industrial liquid electrolyte systems.

3.2. Chronoamperometry curves

Fig. 2 shows the chronoamperometry curves of nickel electrocrystallization on glassy carbon, gold, and nickel electrode surfaces at different step potentials. From Fig. 2(a), (b), and (c), when the step potential is −0.85 to −1.00 V, the *I-t* curves on all substrates show a gradual rise of current with time, reach a maximum value, and then attenuate to a stable value (except the unstable part in the curve for the glassy carbon electrode). In this process, when the deposition time is short, the crystal nucleus size is small, and its growth is controlled by diffusion, that is, the substrate surface undergoes a transience electric double layer charging process to reach a maximum current I_m (current caused by nucleation process) at t_m (t_m is the relaxation time, which is obtained by statistically calculating the raw data of Chronoamperometric curves) [19]. With the gradual extension of deposition time, when the size of crystal nucleus keeps growing and reaches a certain size, the influence of kinetic factors on this process cannot be ignored. At this time, nucleation is no longer a pure diffusion control, but a mixed control of diffusion and other electrochemical reactions [19,23,24]. With the negative shift of the step potential, that is, when the overpotential increases, the peak current I_m increases, and its corresponding t_m becomes shorter, indicating that a higher overpotential increases the nucleation rate and decreases the nucleation induction time. As time elapses, the current tends to be constant. With the negative shift of the step potential, the shorter the nucleation induction time, the higher the maximum nucleation current, indicating that the electrocrystallization of nanocrystalline nickel on the surface of these three electrodes is characterized by three-dimensional nucleation growth under typical diffusion control. Fig. 2(d) compares the *I-t* curves of nanocrystalline nickel electrodeposition in industrial electrolytes at different step potentials and on different substrates. The *I-t* curve for the nickel electrode is significantly more regular than those of the glassy carbon and gold electrodes with the negative shift of the step potential. At a given step potential, the *I-t* curves are similar on different substrates, but the nucleation relaxation time t_m becomes shorter in the order of glassy carbon > gold > nickel electrode. It shows that the different substrates will affect the nucleation overpotential of nickel, and the nickel electrode promotes nickel electrocrystallization nucleation relative to the glassy carbon and gold electrodes. These observations are consistent with the conclusion from the CV curves.

Fig. 2 shows that in the industrial electrolyte, as the deposition potential is negatively shifted and the deposition time is prolonged, the *I-t* curve for glassy carbon electrode becomes irregular and unstable due to smoothing, so the obtained experimental data are less reliable. This can be attributed to the poor adhesion of nanometer-sized nickel grains on the surface of glassy carbon electrode, and the increased heat generated during the deposition due to excessive real current density. As a result, the curve becomes unstable and the nickel deposition layer fall off, and the instability time comes earlier when the potential is negatively shifted. By comparison, the *I-t* curve for the gold electrode is more stable, but the softness of gold makes it difficult to produce a stable real electrode area in the pre-treatment process. That is, under the same conditions, the true current density on the gold electrode can vary. As a result, the *I-t* curves are not very repeatable and appear less regular than those for the nickel electrode. In comparison, the *I-t* curve for the nickel electrode is more stable and reliable than those from the other two electrodes. This is because the electrodeposited layer in this case has the same lattice properties as the nickel substrate, so that their adhesion is significantly stronger. Also, since nickel is harder than glassy carbon and gold, the nickel electrode can guarantee a stable real electrode area after the pretreatment, making the true current density relatively stable under the same conditions. When the step potential is −1.00 V and the deposition time is gradually extended, the time it takes for the nanocrystalline nickel electrodeposited layer to peel from the electrode increased in the order of glassy carbon < gold < nickel. Part of the reason is the increasing adhesion of nickel nanocrystalline grains on the electrodes. Also, excessive current density accelerates the electrodeposition rate of nickel ions on the substrate surface, and the quality of electrodeposited nickel layer is ranked as glassy carbon < gold < nickel electrodes. Finally, the amount of heat generated during nickel deposition increases in the same order, and heating could also induce detachment of the electrodeposited nickel layer [25]. In summary, the gold and nickel electrodes are more suitable as the working electrode in chronoamperometry experiments using the industrial electrolyte system. That is to say, the gold and nickel electrodes are more suitable for scientific research on the electrocrystallization process of nickel in industrial electrolytes.

After processing data from the *I-t* curves in Fig. 2, it can be seen from Table 2 that as the overpotential increases, the relaxation time t_m of the nickel electro-crystallization nucleation on all three surfaces gradually decreases, and the maximum current I_m gradually increases, Moreover, t_m and I_m showed irregular gradations for the glassy carbon and gold electrodes, while the nickel electrode showed regular gradations [16]. The value of t_m (the nucleation relaxation time) for nickel electrocrystallization at the same potential ranks as glassy carbon > gold > nickel electrodes, indicating that the Ni^{2+} crystallization nucleation on the substrate is increasingly promoted in this order. Also, in Table 2 $I_m^2 t_m$ changes in the order of glassy carbon > gold > nickel electrodes at the same potential, and the corresponding $I_m^2 t_m$ value averaged over different potentials also decreases in turn, indicating

Table 2
Data obtained from the *I-t* curves for different electrodes. GCE: glassy carbon electrode.

E/(V)	t_m/(s)			I_m/(A × 10^{-4})			$I_m^2 t_m$/($A^2 \cdot s \times 10^{-5}$)		
	GCE	Au	Ni	GCE	Au	Ni	GCE	Au	Ni
−0.85	43.054	29.204	16.854	−8.6	−9.8	−10.9	3.1843	2.8048	2.0024
−0.90	39.004	17.054	8.003	−13.7	−21.5	−20.6	7.3207	7.8832	3.3962
−0.95	14.954	7.654	4.603	−28.1	−33.9	−29.4	11.8078	8.7961	3.9786
−1.00	5.952	2.803	2.454	−35.4	−38.3	−40.5	7.4588	4.1117	4.0252
Average	–	–	–	–	–	–	7.4429	5.8990	3.3506

decreasing number of nuclei for nickel electrocrystallization as glassy carbon > gold > nickel electrodes at the same potential. In other words, the substrate here affects the number of nuclei in nickel electrocrystallization. The change of $I_m^2 t_m$ among different substrates also depends on the negative shift of the step potential: when the step potential is shifted from −0.85 to −1.00 V, $I_m^2 t_m$ increases for the nickel electrode, while for the glassy carbon and gold electrodes this value first increases and then decreases with the negative shift of step potential, both reaching a maximum value at −0.95 V. Combined with the above results and related literature, we can conclude that $I_m^2 t_m$ first increases and then decreases with the increase of overpotential, and different substrates will affect the potential value corresponding to the maximum value of $I_m^2 t_m$.

The following dimensionless theoretical relationship of transient current in chronoamperometry is derived from the classical SH theoretical model [26]:

Instantaneous nucleation:

$$\frac{I^2}{I_m^2} = 1.9542\frac{t_m}{t}\left\{1 - exp\left[-1.2564\left(\frac{t}{t_m}\right)\right]\right\}^2 \quad (1)$$

Continuous nucleation:

$$\frac{I^2}{I_m^2} = 1.2254\frac{t_m}{t}\left\{1 - exp\left[-2.3367\left(\frac{t}{t_m}\right)^2\right]\right\}^2 \quad (2)$$

where I_m is the peak current and t_m is the peak current time.

The experimental results in Fig. 2 were subjected to dimensionless processing according to Eqs. (1) and (2). From the calculation, the I^2/I_m^2-t/t_m curve is obtained and compared with the theoretical ones for transient and continuous nucleation from the SH model (solid lines in Fig. 3). As shown in Fig. 3, in the experimental potential interval, when $t < t_m$ the curve of glassy carbon electrode is close to the continuous nucleation, while that of $t_m < t < 1.5t_m$ is close to the instantaneous nucleation. For the gold electrode, the curve at $t < t_m$ gradually shifts from continuous nucleation to instantaneous formation. Then, at $t > t_m$, the experimental curve gradually deviates from the instantaneous nucleation curve and tends to be stable. For the nickel electrode, when $t < t_m$, the experimental curve is close to the theoretical curve of continuous nucleation, while that of $t_m < t < 2t_m$ is close to the instantaneous nucleation. Finally, for $t > 2t_m$, the experimental curve gradually deviates from the instantaneous nucleation theoretical curve and tends to be stable. To sum up: the actual nucleation curve for different substrates gradually changes from continuous nucleation to transient nucleation, but the time of the transition is different [20]. So, although the choice of substrate does not change the electrocrystallization mechanism of nickel, it will have an impact on their transition.

Note that the nucleation process of nickel in industrial electrolytes differs from that reported by Li [19] and Gomez et al. [12,14–16], who used glassy carbon electrodes in a conventional electrolyte. Therefore, the electrocrystallization process of nickel nanocrystals is more complicated in industrial electrolytes than in an electrolyte with simple components, such as watt liquid, etc.

3.3. SEM observation

The nanocrystalline nickel deposited on the surface of different electrodes in the industrial electrolytic liquid system by chronoamperometry was observed by SEM. The results are shown in Fig. 4, where panels a, b, and c are the microscopic morphology of nanocrystalline Ni layer deposited at −1.00 V/4 s on glassy carbon, gold, and nickel electrodes, respectively. Panels d and e are the microscopic morphology of nanocrystalline Ni layer deposited at −1.00 V/8 s on gold, and nickel electrodes, respectively. Panel f is the corresponding chronoamperometric curve. In the initial stage of electrodeposition, the

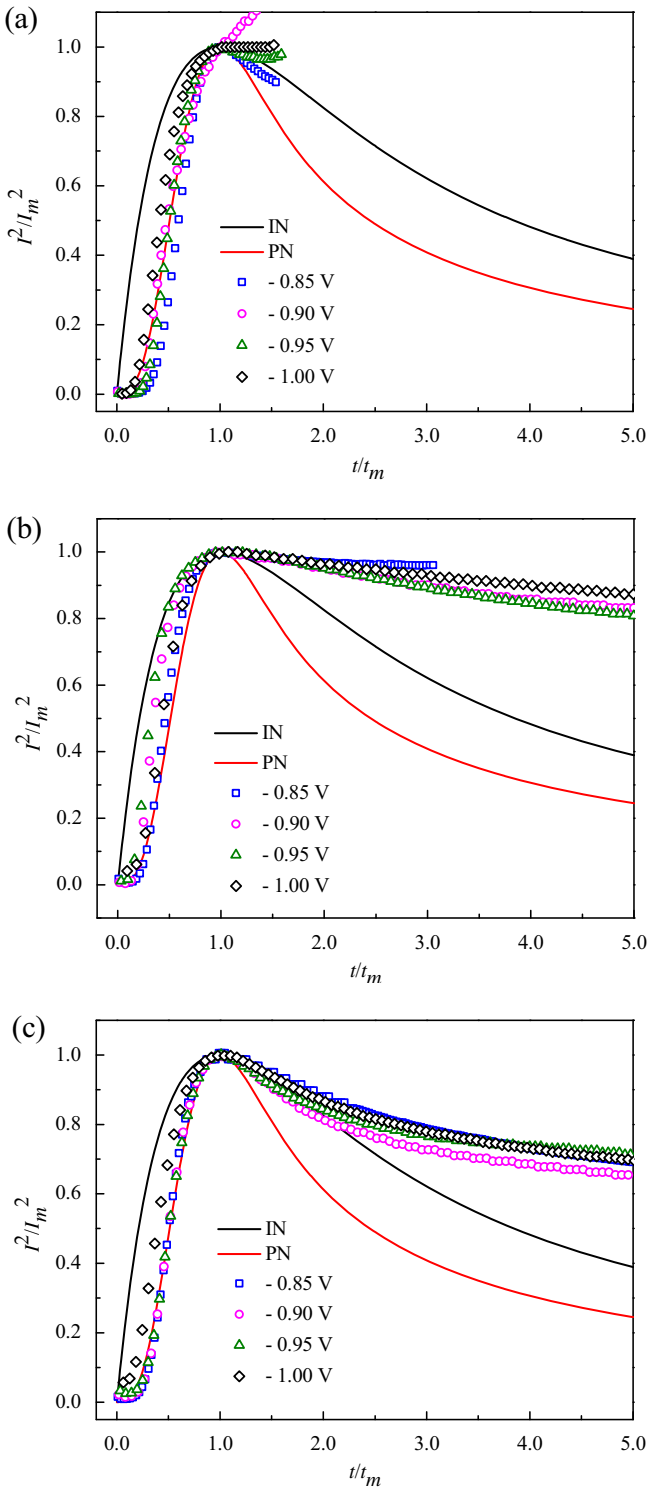

Fig. 3. Comparison of the theoretical dimensionless plots for "instantaneous nucleation" and "progressive nucleation" to the experimental data of nickel nucleation on different substrate materials at potential vs. SCE. (a) Glassy carbon electrode, (b) gold electrode, and (c) nickel electrode. (For interpretation of the references to colour in this figure legend, the reader is referred to the web version of this article.)

deposited metal ions preferentially enter the existing lattice position on the surface of the cathode under the action of the electric field on the surface of the cathode to form a nickel deposition layer (the epitaxial growth region) that is completely aligned with the crystal orientation of the cathode [27]. From the images, the growth morphology of nickel

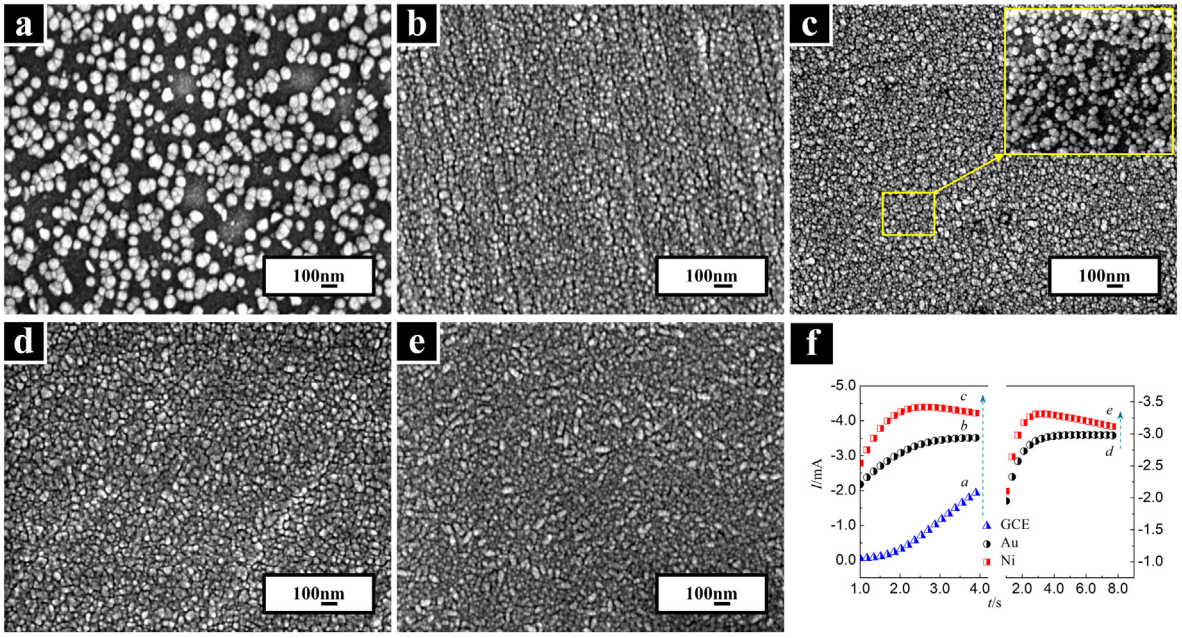

Fig. 4. Micromorphology of nickel deposits on (a) glassy carbon electrode, (b, d) gold electrode and (c, e) nickel electrode at (a, b, c) -1.00 V, 4 s and (d, e) -1.00 V, 8 s. (f) Corresponding chronoamperometric curves. (For interpretation of the references to colour in this figure legend, the reader is referred to the web version of this article.)

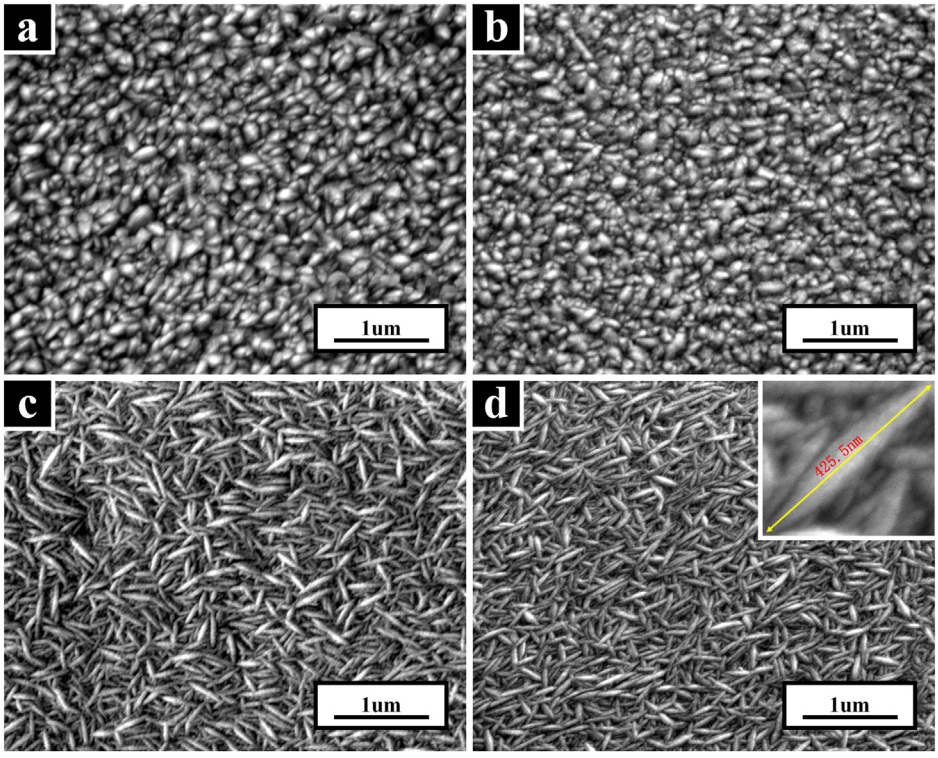

Fig. 5. Micromorphology of nickel deposits on (a, c) gold electrode and (b, d) nickel electrode at (a, b) -0.95 V, 100 s and (c, d) -1.00 V, 100 s. (For interpretation of the references to colour in this figure legend, the reader is referred to the web version of this article.)

electrocrystals clearly is different on the three substrates, due to the different real current density on the electrode surface and the different crystal orientations between the sediment layer and the substrate. The grain size of the deposited nickel changes as glassy carbon > gold > nickel electrode, because the ratio between the rate of actual nucleation and the rate of crystal nucleus growth increases in this order. During the electrocrystallization of nickel, the number of nuclei on the electrode surface increases as nickel < gold < glassy carbon, and the deposition overpotential increased accordingly. Theoretically, the grain size should decrease and the density of the sediment layer should increase in this order. However, the changes in grain size and electrodeposited nickel layer density on the surface of glassy carbon, gold and nickel electrode from Fig. 4 differ from the theory. It can be seen from Fig. 4 f that under the same conditions, the actual current density on the surface of glassy carbon, gold and nickel electrodes increases in turn, so, the grain sizes of the nickel nanocrystals deposited on the surface of

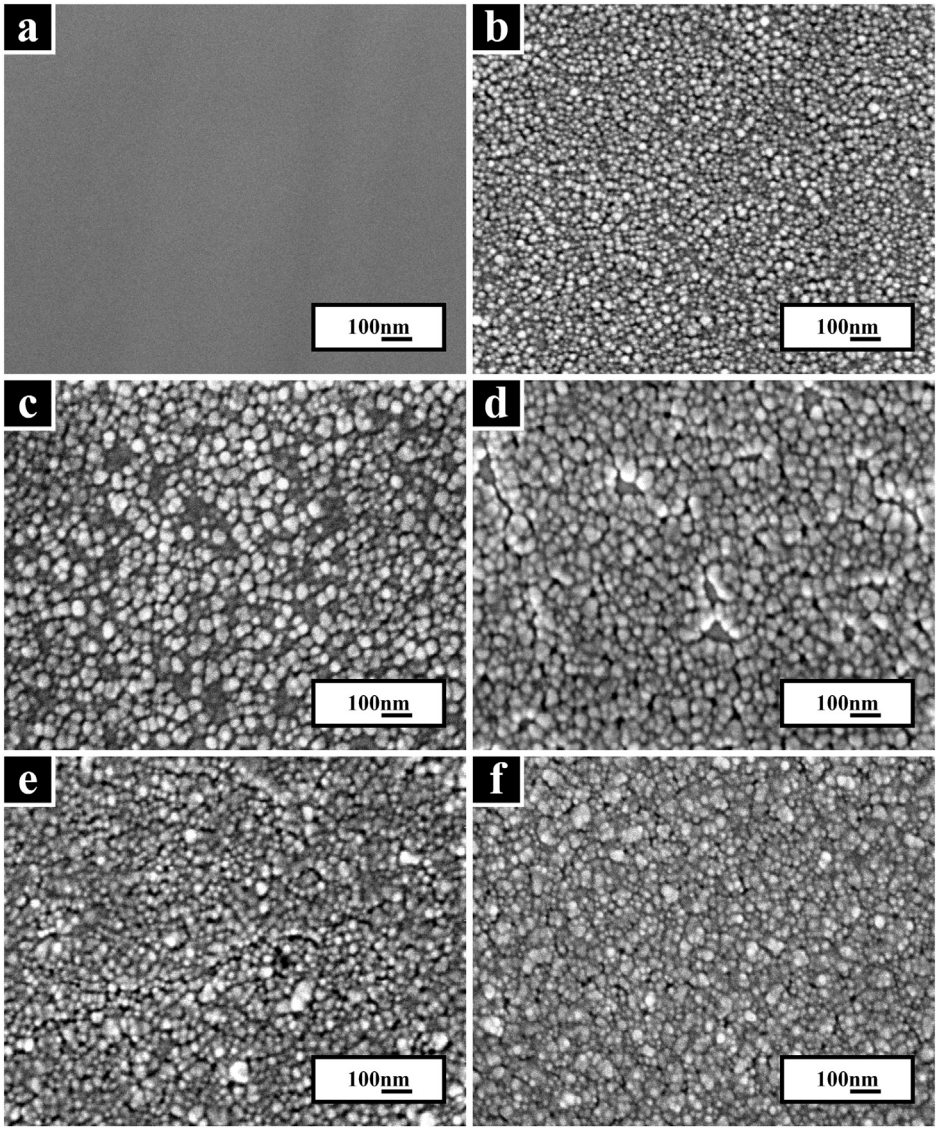

Fig. 6. Micromorphology of nickel deposits on nickel electrodes after (a) 0 s, (b) 2 s, (c) 4 s, (d) 6 s, (e) 8 s, and (f) 10 s (all at −0.90 V).

glassy carbon, gold and nickel electrodes were decreased successively under the same conditions [21]. Since the hardness of gold is less than the hardness of nickel, the polished gold electrode surface still has minute scratches which are unevenly distributed, as well as some impurities that are difficult to remove. The presence of these defects causes the surface of the gold electrode is uneven on micro-scale. The nickel ions will preferentially deposit on the raised part of the electrode surface due to high electric field density at the raised part on electrode surface. The more nickel atoms have electrodeposited at the raised parts, and grain size locality of nickel electro-crystallization has increased. The course of reductive reaction is inhibited due to the relative abundance of the Ni^{2+}. The growth of nickel electro-crystallization is hindered on the detection of concave points around the convex part [28], which results in the uneven distribution of the nanocrystalline nickel particles deposited on the surface of the gold electrode. Regarding the spatial distribution of nickel deposited under the same condition, only about one fifth of the surface of glassy carbon electrode was covered by nickel deposit, while the gold electrode was completely covered with a nickel deposit layer that was not very even. In contrast, the nickel deposit covers the entire surface of nickel electrode uniformly. This difference in the surface distribution of nickel deposit is attributed to various factors, such as the different adhesion force of nickel nanoparticles on the surface, the uneven distribution of defects on the electrode surface, as well as incomplete purification of the electrodes [7].

The nanocrystalline nickel deposited on the surface of gold and nickel electrodes under other chronoamperometry conditions was also observed by SEM. Fig. 5 a and b show the micro morphology of nanocrystalline nickel deposits obtained at −0.95 V/100 s, while c and d are the micro morphology obtained at −1.00 V/100 s. From the figures, the nickel deposit layer completely and uniformly covered the entire surface of both electrodes. After ultrasonic cleaning of the nickel deposit, the surface of the gold electrode partially fell off while the nickel electrode was intact, which is attributed to the increased adhesion of the nickel nanocrystals on these electrodes (being consistent with results obtained by chronoamperometry). Under the same conditions, when the deposition potential is changed from −0.95 V to −1.00 V, the surface morphology of the nickel deposit layer obtained after 100 s of deposition changes from “pyramid” to “rice grain”, that is, the epitaxial growth mode shifts to the fiber texture growth mode. This is because as the deposition potential increases, the grains grow rapidly along their preferred orientation, but grow slowly or not at all in other directions. That is, changing the deposition potential has an effect on the growth morphology of nickel nanocrystals. Therefore, the growth mechanism

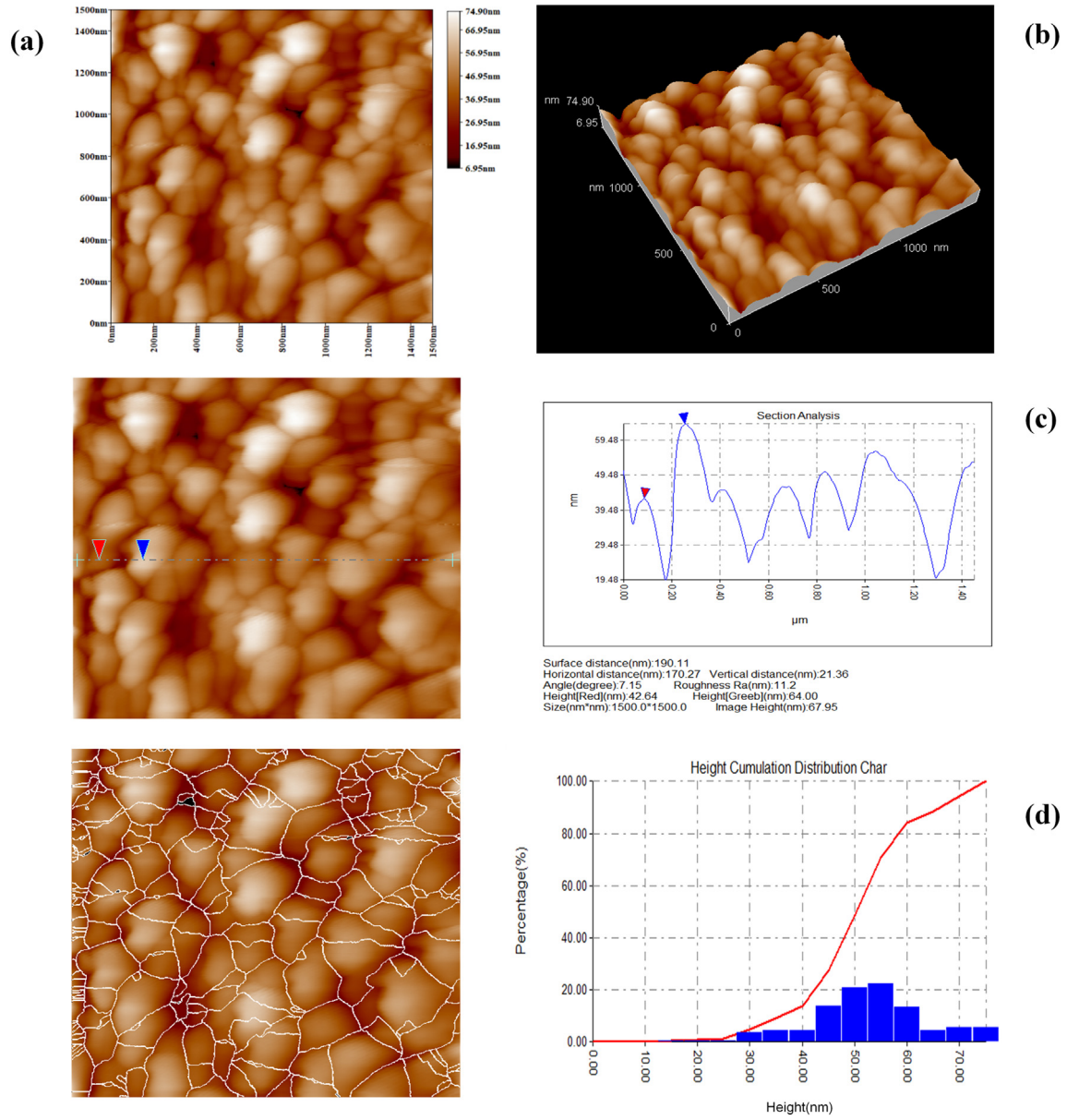

Fig. 7. Tapping mode AFM topographic images of nanocrystalline Ni layer deposited at −0.95 V, 100 s on nickel electrode. (a, b) 2D and 3D topographic images, (c) section analysis diagram, and (d) height cumulation distribution map.

and surface morphology of nickel electrocrystallization in industrial electrolytes will change due to different deposition potentials and deposition times [27]. The growth morphology of nickel electrocrystallization on the surface of gold and nickel electrodes is similar under the same deposition potential, since similar actual current densities were passed through the two electrode surfaces and the orientation difference with the substrate is small. The deposited grain size was smaller on nickel than on the gold electrode, according to the relatively higher ratio between the rate of nucleation on the electrode surface to the rate of nucleus growth on nickel electrode, which is consistent with the conclusions obtained in Fig. 4.

Based on the above findings regarding the electrocrystallization behavior of nanocrystalline nickel in the industrial electrolyte, the nickel electrode was selected as the substrate after optimization, and the step potential was set to −0.90 V. As shown in Table 2, the deposition time at the peak current in the *I-t* curve at −0.90 V was 8.002 s. Therefore, the deposition time for the nickel electrode was set as 0, 2, 4, 6, 8, and 10 s in turn. The resultant SEM images (Fig. 6) confirm the transition in nickel nucleation mechanism from continuous nucleation to instantaneous nucleation [20]. The grain size of nickel nanocrystals changes from non-uniform to uniform with time under the same potential, which is consistent with the transition in growth law from continuous nucleation to instantaneous nucleation as revealed by the chronoamperometry curves.

The nanocrystalline nickel deposited on the surface of nickel electrode in the industrial electrolytic liquid system by chronoamperometry was observed by tapping mode AFM. The results are shown in Fig. 7, where panels a and b are the 2D and 3D topographic images of nanocrystalline Ni layer deposited at −0.95 V/100 s on nickel electrode, while c and d are the section analysis diagram and height cumulation distribution map, respectively. From the figures, the nickel deposit layer completely and uniformly covered the entire surface of nickel electrode and the thickness of the nickel deposit layer is about 80 to 90 nm. Using the AFM image analysis system, the average roughness of the surface of the nickel deposit layer is 8.71 nm, the root mean square roughness is 11.1 nm, the peak-to-peak roughness is 68 nm, the average particle size is 82.88 nm. From the section analysis diagram (Fig. 7 c), we can conclude that the thickness of the deposited layer on the section

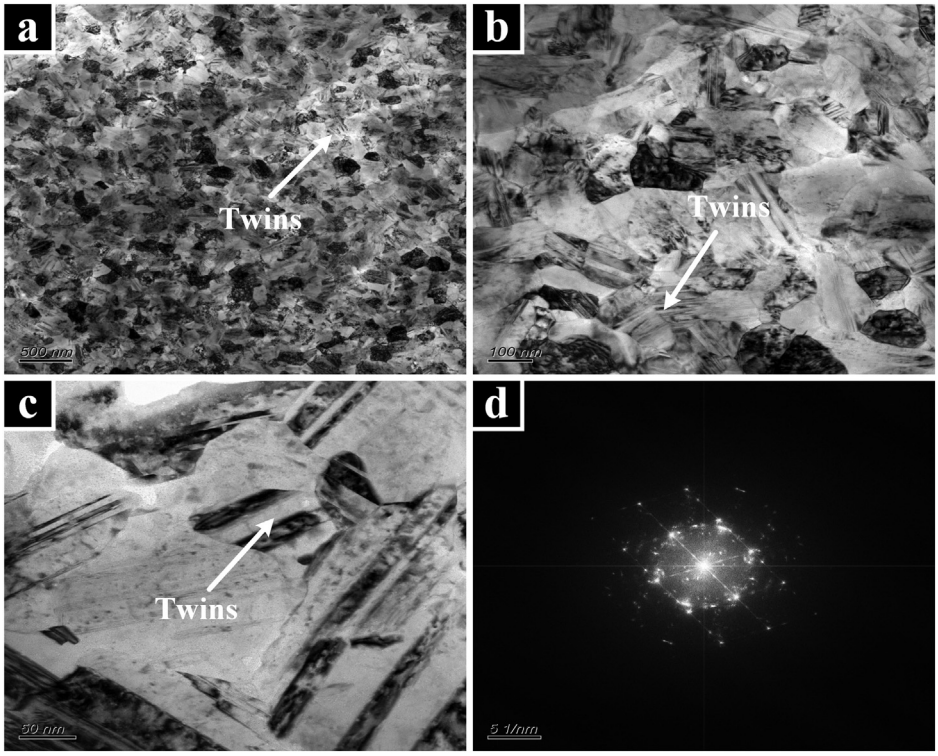

Fig. 8. TEM bright field image and electron diffraction pattern of nickel deposits on gold electrode at −0.95 V, 100 s. (For interpretation of the references to colour in this figure legend, the reader is referred to the web version of this article.)

is between 40 and 65 nm, and Ra is 11.2 nm, further indicating that the nickel deposit layer obtained on the nickel electrode is uniformly distributed. From the height cumulation distribution map (Fig. 7 d), we can conclude that the height of the nickel nanometer grain are conformed to the normal distribution, and most nanometer grain have a height between 45 and 60 nm. This more fully illustrates that the nickel nanometer grain are uniformly distributed on the surface of the nickel electrode [29].

The nanocrystalline nickel deposited on the surface of gold electrode in the industrial electrolytic liquid system by chronoamperometry was observed by TEM. The results are shown in Fig. 8, where panels a, b, and c are the TEM bright field image of nanocrystalline Ni layer deposited at −0.95 V/100 s on gold electrode. It can be seen from the figure that the grain size distribution in the deposited layer is uniform, and the average grain size is about 200 nm, and there are more twin structures inside the grains. Fig. 8d are the transmission electron diffraction (TED) pattern of nanocrystalline Ni layer deposited on gold electrode, from which we can see that the crystal structure of the deposited layer is face-centered cubic (fcc). From the metal crystallography, we can know that the crystal structure of the nickel deposited layer is face-centered cubic [30,31].

4. Conclusions

The nickel electrocrystallization process on different working electrodes was examined in an industrial electrolyte. Voltammetric data show that the initial deposition potentials of nickel shift to the positive direction in the order glassy carbon < gold < nickel electrodes, while the nickel deposition overpotential decreased at the same time. Chronoamperometry results indicated that from the glassy carbon to gold and nickel electrodes, the adhesion of nickel nanoparticles on the electrodes increased, nucleation relaxation time became shorter, and the number of nuclei decreased. As the deposition potential is negatively shifted and the deposition time is prolonged, the *I-t* curves for the nickel and gold electrodes is more stable and reliable than those from the glassy carbon electrodes. Therefore, the glassy carbon electrode is not suitable for prolonged high-potential electrodeposition experiments in complex electrolyte systems, while the gold and nickel electrodes are more suitable for studying industrial electrolyte systems. Chronoamperometric studies combined with SEM show that the choice of deposition substrate does not change the electrocrystallization mechanisms of nickel. From glassy carbon to gold and then nickel electrodes, the electrocrystallization process changes from a three-dimensional continuous nucleation/growth mechanism to a three-dimensional transient nucleation/growth mechanism. When the deposition time is extended from 0 to 10 s, the nickel nanocrystals change from uneven sizes to uniform size. When the deposition time is 100 s, the nanocrystalline nickel deposited on the nickel and gold electrodes has good integrity and uniformity. This was also confirmed in studies using atomic force microscopy and transmission electron microscopy. Moreover, the results of transmission electron microscopy (TEM) show that there are many twins in the nanocrystalline nickel layer deposited on the gold electrode at −0.95 V, 100 s. The electrocrystallization process of nickel is complicated by the complex ionic components in the industrial electrolyte of the nickel sulfide soluble anode/mixed acid system.

References

[1] X. Yang, M. An, Y. Zhang, Electrodeposition behaviors of gold in bath with DMDMH as a complexing agent, Chin, J. Inorg. Chem. 28 (2012) 1145–1150.
[2] F. Yang, L. Huang, S. Xu, Studies on the electrodeposition behaviors of palladium by the actions of additive, Acta Phys. -Chim. Sin. 20 (2004) 463–467.
[3] J. Shi, F. Yang, Z. Tian, Electrocrystallization of cu-Sn alloy on copper electrode surface, Acta Phys. -Chim. Sin. 29 (2013) 2579–2584.
[4] M. Moharana, A. Mallik, Nickel electrocrystallization in different electrolytes: an in-process and post synthesis analysis, Electrochim. Acta 98 (2013) 1–10.
[5] J. Amblard, M. Froment, G. Maurin, N. Spyrellis, E. Trevisan-Souteyrand, Nickel electrocrystallization-from nucleation to textures, Electrochim. Acta 28 (1983) 909–915.
[6] N. Atanassov, S. Vitkova, S. Rashkov, Electrocrystallization of nickel coatings with ⟨211⟩ texture, Surface Technology 13 (1981) 215–223.
[7] S.M. Zhou, Metal Electrodeposition-Principles and Research Methods, Shanghai

Science and Technology Press, Shanghai, 1987, pp. 249–255.
[8] Q.X. Zha, Introduction of Electrode Process Dynamics, Science Press, Beijing, 2001, p. 288.
[9] M.Y. Abyaneh, Extracting nucleation rates from current-time transients (part I): the choice of growth models, J. Electroanal. Chem. 530 (2002) 82–88.
[10] M.Y. Abyaneh, M. Fleischmann, Extracting nucleation rates from current-time transients (part II): comparing the computer-fit and pre-pulse method, J. Electroanal. Chem. 530 (2002) 89–95.
[11] M.Y. Abyaneh, Extracting nucleation rates from current-time transients (part III): nucleation kinetics following the application of a pre-pulse, J. Electroanal. Chem. 530 (2002) 96–104.
[12] E. Gomez, C. Muller, W.G. Proud, Electrodeposition of nickel on vitreous carbon: influence of potential on deposit morphology, J. Appl. Electrochem. 22 (1992) 872–876.
[13] N.V. Sotskaya, L.V. Sapronova, O.V. Dolgikh, Kinetics of the nucleation and growth of nickel particles in α-alanine-containing electrolytes, Prot. Met. Phys. Chem. Surf. 50 (2014) 22–26.
[14] C. Tan, Fabrication of Nickel, Copper Matrix Composite Coatings and their Electrochemical Behaviors, Central South University, 2008.
[15] N.V. Sotskaya, L.V. Sapronova, O.V. Dolgikh, Kinetics of nickel electrocrystallization from serine-containing electrolytes, Rus. J. Electrochem. 50 (2014) 1137–1141.
[16] Y. Liu, C. Tan, Z. Jia, Effect of copper ions on behavior of nickel electro-crystallization on glassy carbon electrode, J. Central South University (Science and Technology) 41 (2010) 144–149.
[17] Y. Zhang, B. Pan, The effect of valine on the process of nickel electrocrystallization on glassy carbon electrode, J. Electroanal. Chem. 796 (2017) 43–48.
[18] F. Lantelme, A. Seghiouer, A. Derja, Model of nickel electrodeposition from acidic medium, J. Appl. Electrochem. 28 (1998) 907–913.
[19] C. Li, X. Li, Z. Wang, Mechanism of electrocrystallization of nickel in sodium citrate solution, J. Central South University (Science and Technology) 46 (2015) 2797–2803.
[20] Y.T. Xu, Y.J. Dai, W. Zhang, T.D. Xia, Microstructure and texture evolution of electrodeposited coatings of nickel in the industrial electrolyte, Surf. Coat. Technol. 330 (2017) 170–177.
[21] N.P. Wasekar, A.P. O'Mullane, G. Sundararajan, A new model for predicting the grain size of electrodeposited nanocrystalline nickel coatings containing Sulphur, phosphorus or boron based on typical systems, J. Electroanal. Chem. 833 (2019) 198–204.
[22] K. Gong, Y.X. Hua, C.Y. Xu, Q.B. Zhang, Y. Li, J.J. Ru, Y.F. Jie, Electrodeposition behavior of bright nickel in air and water-stable betaine·HCl-ethylene glycol ionic liquid, Trans. Nonferrous Metals Soc. China 25 (2015) 2458–2465.
[23] M. Gu, F.Z. Yang, L. Huang, S.B. Yao, S.M. Zhou, Effect of chloride ion on electrocrystallization of copper on glass carbon electrode, Acta Chim. Sin. 60 (2002) 1946–1950.
[24] A.I. Danilov, E.B. Molodkina, Y.M. Polukarov, Initial stages of the copper electrocrystallization from a sulfuric acid electrolyte: chronoamperometry at a platinum ring-disk electrode, Russ. J. Electrochem. 36 (2000) 1236–1244.
[25] X.Y. Li, The experimental research on CNC pulse electric plating, Nanjing Agricultural University, Nanjing, 2014.
[26] B. Scharifker, G. Hills, Theoretical and experimental studies of multiple nucleation, Electrochim. Acta 28 (1983) 879–889.
[27] S. Akinobu, N. Homuro, S. Masato, H. Yakichi, Microstructural development of an electrodeposited Ni layer, Thin Solid Films 518 (2010) 5153–5158.
[28] T. Watanabe, Z.P. Chen, G. Yang (Eds.), Written, Nano-Plating, Chemical Industry Press, Translated, Beijing, 2007.
[29] E. Rahimi, A. Davoodi, A.R.K. Rashid, Characterization of screw dislocation-driven growth in nickel micro-nanostructure electrodeposition process by AFM, Mater. Lett. 210 (2018) 341–344.
[30] F.Y. Ouyang, K.H. Yang, L.P. Chang, Effect of film thickness and Ti interlayer on structure and properties of Nanotwinned cu thin films, Surface & Coatings Technology 350 (2018) 848–856.
[31] Y. Li, Corrosion Behaviors of Nonocrystalline Nickel and Nickel-Chromium Composite Coatings Synthesized by Jet Electrodeposition, Harbin Engineering University, 2013.